Shedding Light on Selenium Biomineralization: Proteins Associated with Bionanominerals[▽]

Markus Lenz,[1,2]* Boris Kolvenbach,[1] Benjamin Gygax,[3] Suzette Moes,[4] and Philippe F. X. Corvini[1,5]

Institute for Ecopreneurship, University of Applied Sciences Northwestern Switzerland (FHNW), School of Life Sciences, Gründenstrasse 40, 4132 Muttenz, Switzerland[1]; Sub-Department of Environmental Technology, Wageningen University, 6700 EV Wageningen, The Netherlands[2]; Institute for Chemistry and Bioanalytics, University of Applied Sciences Northwestern Switzerland (FHNW), School of Life Sciences, Gründenstrasse 40, 4132 Muttenz, Switzerland[3]; Biozentrum, University of Basel, Klingelbergstrasse 50/70, 4056 Basel, Switzerland[4]; and School of the Environment, Nanjing University, 22 Hankou Rd., Nanjing 210093, People's Republic of China[5]

Selenium-reducing microorganisms produce elemental selenium nanoparticles with particular physicochemical properties due to an associated organic fraction. This study identified high-affinity proteins associated with such bionanominerals and with nonbiogenic elemental selenium. Proteins with an anticipated functional role in selenium reduction, such as a metalloid reductase, were found to be associated with nanoparticles formed by one selenium respirer, *Sulfurospirillum barnesii*.

Certain anaerobic microorganisms utilize selenite and selenate as terminal electron acceptors for respiration and growth (dissimilatory reduction), producing elemental selenium, either as internal accumulations that can be released to the medium or extracellularly (5, 11, 12). Despite these differences in mechanism of formation, biogenic elemental selenium generally does not form large crystals but rather spherical nanoparticles (7, 8, 12). It has been hypothesized that biogenic selenium nanoparticles can be stabilized against crystallization due to the presence of proteins (5), yet hitherto, no proteins associated with nanoparticles of respiratory selenium reducers have been identified. This study investigated such proteins using two dissimilatory selenium reducers, *Bacillus selenatarsenatis* (DSMZ 18680) and *Sulfurospirillum barnesii* (DSMZ 10660). For comparison, *Rhodospirillum rubrum* (DSMZ 467), which can induce selenium precipitation, although not in a dissimilatory manner, was investigated.

Microorganisms were grown anaerobically in media according to the culture collection (DSMZ) with the addition of 20 mM selenate (*B. selenatarsenatis*, *S. barnesii*) or 1 mM selenite (*R. rubrum*). *B. selenatarsenatis* was first pregrown aerobically without the addition of selenium and transferred to anaerobic medium during the exponential growth phase. *S. barnesii* was grown using a N_2-CO_2 (80:20 [vol/vol]) headspace instead of N_2. *R. rubrum* was grown under light. Selenium nanoparticles were harvested in all batches in the late stationary phase, since formation in *R. rubrum* occurs during that phase (5). As a control, lysed cells and culture medium were incubated with conventionally synthesized elemental selenium (hereinafter referred to as "nonbiogenic") (Sigma Aldrich, Buchs, Switzerland). For this, pure cultures were grown in the absence of selenium oxyanions and subsequently lysed by means of an ultrasonic probe (Labsonic M; Sartorius, Tagelswangen, Switzerland).

High-affinity proteins associated with elemental selenium (biogenic, nonbiogenic) were isolated from low-affinity/nonassociated proteins and residual biomass using density-based centrifugation in sodium polytungstate solution (SPTS) modified according to references 10 and 13. Batch medium (50 ml) was centrifuged (30 min; 5,000 × g), and pellets were washed twice with Tris buffer (50 mM, pH 7.2) and transferred to the top of SPTS (density, 3 g/ml) (TC Tungsten Compounds, Grub, Germany). Samples were then subjected to low-speed centrifugation (30 min, 2,000 × g), the supernatants containing low-affinity/nonassociated proteins and biomass were discarded, and the pellets were transferred into tubes containing fresh SPTS. Controls using biomass grown without selenium received the same treatment. Since no visible pellet was formed in the latter, 200 µl of SPTS was transferred instead. Centrifugation (five repetitions) was followed by washing with Tris-buffer (seven repetitions) to exhaustively remove remaining SPTS.

Sodium dodecyl sulfate-polyacrylamide gel electrophoresis (SDS-PAGE) was used to separate proteins following standard protocols (6). Sypro orange (limit of detection [LOD], 1 to 2 ng/band) (Fig. 1) and colloidal blue staining (LOD, <10 ng/band) revealed a number of protein bands for all microbial species used. Protein bands were found to be most abundant at apparent molecular masses of between 23 and 60 kDa (*B. selenatarsenatis*) (Fig. 1A), 61 and 69 kDa (*R. rubrum*) (Fig. 1B) and 52 and 80 kDa (*S. barnesii*) (Fig. 1B).

For mass spectrometry (MS) analysis, colloidal blue-stained bands were excised, reduced with dithiothreitol (10 mM, 2 h, 37°C), alkylated with iodoacetamide (50 mM, 15 min, at room temperature and in darkness), trypsin digested (125 ng trypsin,

* Corresponding author. Mailing address: Institute for Ecopreneurship, University of Applied Sciences Northwestern Switzerland (FHNW), School of Life Sciences, Gründenstrasse 40, 4132 Muttenz, Switzerland. Phone: 41 614 674 791. Fax: 41 614 674 290. E-mail: Markus.Lenz@fhnw.ch.
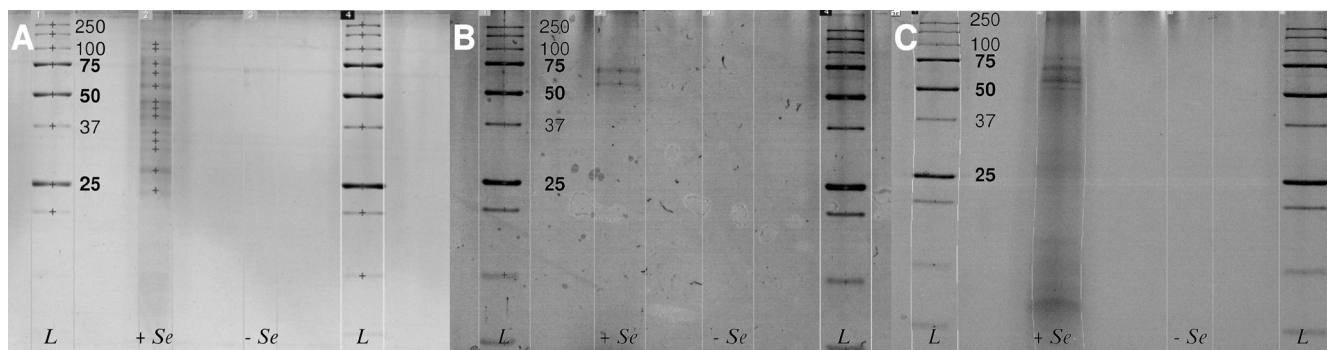
FIG. 1. SDS-PAGE gel images (Sypro orange stain) of proteins associated with biogenic selenium nanoparticles (+ *Se*) and controls (− *Se*) produced by *Bacillus selenatarsenatis* (A), *Rhodospirillum rubrum* (B), and *Sulfurospirillum barnesii* (C) after density-based centrifugation. Molecular size standards (*L*) are in kilodaltons.

sequencing grade, 18 h, 37°C), and concentrated in a SpeedVac concentrator. Capillary liquid chromatography-electrospray ionization-tandem mass spectrometry (LC-ESI-MS/MS) was conducted with an Orbitrap FT hybrid instrument (Thermo Finnigan, San Jose, CA) (17). The MS/MS spectra were searched against the NCBI data bank (using the Matrix Science portal) by applying the following constraints: carbamidomethyl cysteine as fixed and N-acetylation and oxidized methionine as variable modifications; tryptic specificity allowing two missed cleavages; peptide tolerance, 10 ppm; MS/MS tolerance, 0.6 Da; taxonomy setting, bacteria. The significance threshold was set to 0.05. The search output was filtered in a stringent manner, omitting all proteins with less than four peptides matched and proteins with molecular weights outside $100\% \pm 20\%$ of the apparent molecular weight determined by SDS.

Our results allowed for the first time a qualitative characterization of the high-affinity protein fraction associated with selenium bionanominerals of different microbial origins. For all microorganisms used here, a plenitude of proteins with diverse cellular functions were identified (Table 1). Furthermore, we could demonstrate that nonbiogenic selenium, as well, associates with a number of proteins produced by dissimilatory selenium reducers. Taking into account the total number of proteins expressed in the studied organisms, it is striking that several proteins were found on both biogenic and nonbiogenic particles. For silver nanoparticles in contact with *Escherichia coli* cell extracts, it has been shown that proteins associated did not simply reflect the most abundant proteins but instead are due to higher affinities of some proteins to the particles (18). In this regard, it is most striking that the protein with the highest number of peptides matched in this study was the so-called "metalloid reductase RarA" found on both biogenic (*S. barnesii*) and nonbiogenic selenium nanoparticles (Table 1). Numerous peptide motifs, so-called aptamers, have to date been described to specifically bind inorganic nanomaterials, among others, chalcogen-based (CdS, PbS, ZnS) and metallic (Au, Ag, Si, etc.) nanomaterials, yet not elemental selenium (see reference 16 and references therein). It may thus well be that the metalloid reductase RarA found in this study contains a natural peptide motif conferring its high affinity to elemental selenium. Such peptide motifs are of high interest, since they can be used to bind elemental selenium surfaces in particular applications, e.g., in bioremediation. Here, a current

technically unresolved challenge is to remove the nanosized biogenic selenium from the aqueous phase (7). Although its name suggests a selenate-reducing enzymatic activity, unfortunately no further information is available at present regarding the enzymatic characterization of this protein. A role as outer membrane porin can be anticipated from sequence similarities with porins from closely related *Sulfurospirillum deleyianum* (59% identity) and *Geobacter lovleyi* (49% identity, NCBI BLAST). It is thus possible that the metalloid reductase found here is involved in the initial uptake of selenate to the periplasm, where other selenate reductases have been found (15).

Furthermore, we were able to identify proteins with additional anticipated functional roles in selenium reduction in spatial association with the formed bionanominerals. Such proteins include, next to the metalloid reductase RarA, proteins involved in electron transport during microbial respiration, peptides with reactive thiol functional groups, and enzymes involved in reactive oxygen species degradation (Table 1).

For *S. barnesii*, we first observed respiratory electron transport chain proteins associated with the bionanominerals, i.e., a nickel-dependent hydrogenase and an aldehyde ferredoxin oxidoreductase. It can thus be interpreted that electrons necessary for reduction of selenate can be supplied by the hydrogenase, and this mechanism has been described for microbial reduction of other toxic oxyanions (1). Electrons can then be transferred via ferredoxin, as has been shown for selenate reduction in *Synechocystis* (9) and selenite reduction in *Clostridium* (19).

Selenite can be reduced to elemental selenium by reaction with reactive thiol groups of proteins/peptides in the so called "Painter-type" reaction, which has been suggested as a general microbial detoxification reaction to oxyanions (3). The latter idea might be further supported by the present study, since we were able to identify peroxiredoxins in *B. selenatarsenatis*, which can contain such catalytic cysteine-thiols (2, 14). In addition to reacting via their thiol, functional groups, the peroxiredoxins found here (peroxiredoxin, alkyl hydroperoxide reductase) can have a further general role in reaction to toxic selenium oxyanions, since they are involved in degradation of reactive oxygen species. These, among other products, are generated during the latter Painter-type reactions (3, 4). The

TABLE 1. Proteins identified by LC-ESI-MS/MS associated with biogenic and nonbiogenic elemental selenium[a]

Organism	Protein name (homologous organism)	GI no.	Protein score[b]	No. of peptides matched	Protein mass (Da)	% Apparent mass[c]	Biogenic Se	Nonbiogenic Se	Both
Bacillus selenatarsenatis	30S ribosomal protein S3 (Anoxybacillus flavithermus WK1)	212637960; 89100343; 169830024	442	17	24,384	98	✓		
	Phosphopyruvate hydratase (Anoxybacillus flavithermus WK1)	212640334; 149183684; 71907983; 241888482	409	9	46,371	97	✓		
	Translation elongation factor Tu (Enterococcus casseliflavus EC30)	257866523; 270341159; 138893783; 30018378; 118443068; 118602795; 16077181; 89100352; 126654355; 56961930; 172056138; 293375387; 260588991; 229542206	327	19	43,187	90	✓		
	30S ribosomal protein S4 (Bacillus coahuilensis m4-4)	205374494; 89100095; 226313743	296	11	23,098	100	✓		
	Inositol-5-monophosphate dehydrogenase (Bacillus sp. strain NRRL B-14911)	89100965; 18311258; 212637858; 15612583; 56418544	281	14	52,973	88	✓		
	Enolase (Bacillus coagulans 36D1)	229543256; 260223073; 167629687	230	5	46,803	98	✓	✓	
	Hypothetical protein CLOLEP_03947 (Clostridium leptum DSM 753)	160935071	218	15	44,341	92	✓		
	Delta-1-pyrroline-5-carboxylate dehydrogenase (Geobacillus sp. strain Y4.1MC1)	255332760	195	5	56,724	95	✓		
	Acetate/propionate kinase (Bacillus sp. strain NRRL B-14911)	89100072	193	8	43,214	90	✓		
	Enoyl-(acyl carrier protein) reductase (Bacillus sp. strain NRRL B-14911)	89100163; 229554841	188	4	29,402	118	✓		
	RecA protein (Leptospirillum rubarum)	124514183; 220934461	178	5	38,792	81	✓	✓	
	Dihydrolipoamide dehydrogenase (Bacillus subtilis subsp. subtilis 168)	16078525; 157692912	168	5	49,873	83	✓		
	ATP-dependent Clp protease proteolytic subunit (Bacillus coahuilensis m4-4)	205375127; 89098789	151	7	21,941	95	✓		
	Hypothetical protein CLOLEP_01281 (Clostridium leptum DSM 753)	160932446	136	7	53,365	89	✓		
	Naphthoate synthase (Staphylococcus aureus subsp. aureus Mu50)	15924035	126	4	30,620	102	✓		
	Alkyl hydroperoxide reductase (large subunit) (Bacillus subtilis subsp. subtilis 168)	16081062; 172059003; 239814820	123	5	55,125	92	✓		
	Seryl-tRNA synthetase (Bacillus halodurans C-125)	15612587; 89100960	121	6	48,625	81	✓	✓	
	Glyceraldehyde-3-phosphate dehydrogenase (Bacillus halodurans C-125)	15616122; 52081962; 89098795	121	5	36,078	98	✓		
	1-Pyrroline-5-carboxylate dehydrogenase (Anoxybacillus flavithermus WK1)	212638098; 89097081; 149182115; 16080830	118	4	56,870	95	✓		
	NADH dehydrogenase/alkyl hydroperoxide reductase (Brevibacillus brevis)	226311081	116	5	54,993	92	✓		
	Clp protease, ATP-binding subunit ClpX (Bacillus cellulosilyticus DSM 2522)	283847485; 261405360; 288553619	115	4	47,274	98	✓		
	Ribosomal protein S4 (Lactobacillus casei ATCC 334)	116494737	114	4	23,292	101	✓		
	Acetate kinase (Bacillus anthracis Ames)	30264711; 30022712; 157693336; 16079999	112	4	43,234	90	✓	✓	
	Hypothetical protein STRINF_00550 (Streptococcus infantarius)	171778571	111	4	22,964	100	✓		
	Ornithine-oxoacid transaminase (Bacillus sp. strain NRRL B-14911)	89100262	110	4	43,745	118	✓		
	50S ribosomal protein L1 (Bacillus clausii KSM-K16)	56961920	99	4	24,894	100	✓		
	Ribosomal protein S9 (Bacillus selenitireducens MLS10)	163764753	99	4	25,000	100	✓		
	Peroxiredoxin (Listeria grayi DSM 20601)	229557407; 239826003	82	5	21,050	92	✓	✓	
	Transcription termination factor Rho (Bacillus amyloliquefaciens FZB42)	154687823; 126652575; 89095596	76	4	48,669	81	✓		
	Hypothetical protein ANACAC_02873 (Anaerostipes caccae DSM 14662)	167748129	52	4	25,800	103	✓		

Organism	GI no. (accession)[a]	Protein (organism)	Score[b]	Peptides	Apparent mass	% mass[c]			
	172057846; 89101193	Translation initiation factor IF-2 (*Exiguobacterium sibiricum* 255-15)	136	4	79,473	110		✓	✓
	89100205; 149776882; 30018515; 157363182; 3832729 6; 116250; 444101	Chaperonin GroEL (*Bacillus* sp. strain NRRL B-14911)	640	22	57,270	108	✓		✓
Rhodospirillum rubrum	83593644	NADH peroxidase (*Rhodospirillum rubrum* ATCC 11170)	237	6	58,867	85	✓	✓	
	83592560; 39933255	ATP synthase F1, alpha subunit (*Rhodospirillum rubrum* ATCC 11170)	185	5	55,163	90	✓		
	83594884	Molecular chaperone DnaK (*Rhodospirillum rubrum* ATCC 11170)	186	5	68,805	100	✓		
	83591926; 75676377	Chaperonin GroEL (*Rhodospirillum rubrum* ATCC 11170)	461	16	57,657	96	✓		✓
	83594896	Uroporphyrinogen III synthase HEM4 (*Rhodospirillum rubrum* ATCC 11170)	227	5	74,928	109			
Sulfurospirillum barnesii	118474584; 15792577	Polynucleotide phosphorylase/polyadenylase (*Campylobacter fetus* subsp. *fetus* 82-40)	165	4	80,155	100	✓		
	268679733	Nickel-dependent hydrogenase large subunit (*Sulfurospirillum deleyianum* DSM 6946)	130	4	64,987	109	✓		✓
	34558143	Aldehyde ferredoxin oxidoreductase (*Wolinella succinogenes* DSM 1740)	99	5	62,377	95	✓		✓
	15800166; 147989; 15641925	Trigger factor (*Escherichia coli* O157:H7 EDL933)	933	35	48,163	104		✓	✓
	223404	Protein S1 (*Escherichia coli*)	399	10	61,236	96			✓
	15800202	Heat shock protein 90 (*Escherichia coli* O157:H7 EDL933)	304	8	71,374	83			✓
	42144	Unnamed protein product (*Escherichia coli*)	144	4	54,682	108		✓	✓
	148556092	TonB-dependent receptor, plug (*Sphingomonas wittichii* RW1)	137	5	67,898	100			✓
	15791942	Aspartate kinase (*Campylobacter jejuni* subsp. *jejuni* NCTC 11168)	111	4	42,820	100			✓
	3599924	GroEL/HSP60 homolog (*Lawsonia intracellularis*)	93	6	58,740	100			✓
	23394982; 15799694; 1943057; 4928208; 169832197; 154175431; 157738395; 149195246; 34556917; 152993455; 15644739; 237751747; 15792097; 91775104; 268679982	Metalloid reductase RarA (*Sulfurospirillum barnesii*)	960	69	48,133	104	✓	✓	✓
	34556744; 187711187; 1421648; 2624772; 438187; 268679392; 21673365; 154148819; 397869; 18308142; 183674907; 183675214; 125490781; 330875 73; 110638228; 54299860; 57242681	Molecular chaperone DnaK (*Escherichia coli* O157:H7 EDL933)	476	18	69,130	116			✓
		Chaperonin GroEL (*Wolinella succinogenes* DSM 1740)	420	19	57,651	87			✓
	15791493; 86160765; 15612127; 86606753; 15644360; 162751865; 193214589; 115374787	F0F1 ATP synthase subunit alpha (*Campylobacter jejuni* subsp. *jejuni* NCTC 11168)	265	8	54,824	95			✓
	150003021; 57167939	Inosine-5-monophosphate dehydrogenase (*Bacteroides vulgatus* ATCC 8482)	121	5	51,890	83			✓

[a] For matches relating to homologous proteins in different organisms, all accession numbers (GI numbers) are given, yet only the organism with the highest ion score is mentioned. Proteins with an anticipated role in selenium reduction are highlighted in gray.

[b] A protein score greater than 42 is considered significant ($P < 0.05$).

[c] % Apparent mass, percentage of the apparent mass as determined by SDS.

same general detoxification role applies to NADH peroxidase found in the nonrespiratory selenium reducer *R. rubrum*.

This study shows that selenium nanoparticles can be associated with a plenitude of high-affinity proteins, despite their microbial origin and/or biogenic character. It is important to note that identification of proteins associated with selenium nanoparticles critically depends on the successful isolation of proteins associated intrinsically from adventitiously associated proteins that are potentially copurified in the density-based centrifugation in SPTS. In this regard, the modification of the centrifugation procedure as applied in this study allowed us first to definitively distinguish between these protein fractions, since selenium-free controls did not show any protein bands in the SDS gels (Fig. 1). Indisputably, the protein modification on the selenium particles will change the physicochemical properties of the selenium solid to some extent and, in consequence, influence the environmental fate of selenium, as has been demonstrated for other bionanominerals (10). Consequently, this study represents a very first step toward understanding the mechanisms underlying the formation of such associations. The high-affinity proteins identified here might be used to design specific probes for, e.g., immunofluorescence or immunoelectron microscopy to further study and visualize the mechanisms of nanoparticle formation. On one hand, owing to the high importance of selenium in animal and human health, there is a clear need to further study the association of the protein fraction to nanoparticles, e.g., by proteomic analysis focusing on expression of proteins/enzymes found here. On the other hand, future studies should also consider the dissociation or biodegradation of the proteic fraction on selenium (or other bionanominerals), hence opening a fascinating yet challenging future field of interdisciplinary biogeochemical research.

REFERENCES

1. **De Luca, G., P. de Philip, Z. Dermoun, M. Rousset, and A. Vermeglio.** 2001. Reduction of technetium(VII) by *Desulfovibrio fructosovorans* is mediated by the nickel-iron hydrogenase. Appl. Environ. Microbiol. **67:**4583–4587.
2. **Georgiou, G., and L. Masip.** 2003. An overoxidation journey with a return ticket. Science **300:**592–594.
3. **Harrison, J. J., H. Ceri, and R. J. Turner.** 2007. Multimetal resistance and tolerance in microbial biofilms. Nat. Rev. Microbiol. **5:**928–938.
4. **Kessi, J., and K. W. Hanselmann.** 2004. Similarities between the abiotic reduction of selenite with glutathione and the dissimilatory reaction mediated by *Rhodospirillum rubrum* and *Escherichia coli*. J. Biol. Chem. **279:**50662–50669.
5. **Kessi, J., M. Ramuz, E. Wehrli, M. Spycher, and R. Bachofen.** 1999. Reduction of selenite and detoxification of elemental selenium by the phototrophic bacterium *Rhodospirillum rubrum*. Appl. Environ. Microbiol. **65:**4734–4740.
6. **Laemmli, U. K.** 1970. Cleavage of structural proteins during the assembly of the head of bacteriophage T4. Nature **227:**680–685.
7. **Lenz, M., M. Smit, P. Binder, A. C. Van Aelst, and P. N. L. Lens.** 2008. Biological alkylation and colloid formation of selenium in methanogenic UASB reactors. J. Environ. Qual. **37:**1691–1700.
8. **Lenz, M., A. C. Van Aelst, M. Smit, P. F. X. Corvini, and P. N. L. Lens.** 2009. Biological production of selenium nanoparticles from waste waters. Adv. Mater. Res. **71–73:**721–724.
9. **Marteyn, B., F. Domain, P. Legrain, F. Chauvat, and C. Cassier-Chauvat.** 2009. The thioredoxin reductase-glutaredoxins-ferredoxin crossroad pathway for selenate tolerance in *Synechocystis* PCC6803. Mol. Microbiol. **71:**520–532.
10. **Moreau, J. W., et al.** 2007. Extracellular proteins limit the dispersal of biogenic nanoparticles. Science **316:**1600–1603.
11. **Narasingarao, P., and M. M. Haggblom.** 2007. Identification of anaerobic selenate-respiring bacteria from aquatic sediments. Appl. Environ. Microbiol. **73:**3519–3527.
12. **Oremland, R. S., et al.** 2004. Structural and spectral features of selenium nanospheres produced by Se respiring bacteria. Appl. Environ. Microbiol. **70:**52–60.
13. **Pearce, C. I., et al.** 2009. Investigating different mechanisms for biogenic selenite transformations: *Geobacter sulfurreducens*, *Shewanella oneidensis* and *Veillonella atypica*. Environ. Technol. **30:**1313–1326.
14. **Poole, L. B.** 2005. Bacterial defenses against oxidants: mechanistic features of cysteine-based peroxidases and their flavoprotein reductases. Arch. Biochem. Biophys. **433:**240–254.
15. **Schröder, I., S. Rech, T. Krafft, and J. M. Macy.** 1997. Purification and characterization of the selenate reductase from *Thauera selenatis*. J. Biol. Chem. **272:**23765–23768.
16. **Shiba, K.** 2010. Exploitation of peptide motif sequences and their use in nanobiotechnology. Curr. Opin. Biotechnol. **21:**412–425.
17. **Vaupotic, T., P. Veranic, P. Jenoe, and A. Plemenitas.** 2008. Mitochondrial mediation of environmental osmolytes discrimination during osmoadaptation in the extremely halotolerant black yeast *Hortaea werneckii*. Fungal Genet. Biol. **45:**994–1107.
18. **Wigginton, N. S., et al.** 2010. Binding of silver nanoparticles to bacterial proteins depends on surface modifications and inhibits enzymatic activity. Environ. Sci. Technol. **44:**2163–2168.
19. **Yanke, L. J., R. D. Bryant, and E. J. Laishley.** 1995. Hydrogenase I of *Clostridium pasteurianum* functions as a novel selenite reductase. Anaerobe **1:**61–67.